Nuclear Instruments and Methods in Physics Research B 269 (2011) 2781–2785

Contents lists available at SciVerse ScienceDirect

Nuclear Instruments and Methods in Physics Research B

journal homepage: www.elsevier.com/locate/nimb

Stochastic simulation of track density in nuclear track detectors for ^{10}B measurements in autoradiography

G. Saint Martin [a,*], A. Portu [a,b], G.A. Santa Cruz [a], O.A. Bernaola [a]

[a] Comisión Nacional de Energía Atómica, Av. Gral. Paz 1499, San Martín, Buenos Aires, Argentina
[b] Consejo Nacional de Investigaciones Científicas y Técnicas (CONICET), Argentina

ARTICLE INFO

Article history:
Received 14 February 2011
Received in revised form 29 August 2011
Available online 8 September 2011

Keywords:
Autoradiography image
Stochastic simulation
Track density
Standard material
BNCT

ABSTRACT

A standard material with a known amount of ^{10}B has to be used as a reference for a quantitative evaluation of boron concentration in autoradiography images of tissue samples. However, the yield of detected charged particles is conditioned upon certain parameters, such as the critical angle, which are determined by the physical properties of the sample material as well as the particle type and energy. A stochastic model was developed to simulate the process of particle emission in the sample and the resultant production of tracks in a polycarbonate detector in contact with it. The model was then applied to study the influence of the sample material on the final track density, from a theoretical point of view. Liver tissue, borated aqueous solutions and silicon boron doped wafers were considered as sample materials. Using a borated aqueous solution as a reference material is acceptable for evaluating tissue samples under certain conditions. The value of track density calculated with the model for 50 ppm borated aqueous solution was compared to analytical calculations and to experimental measurements in polycarbonate track detector. Differences between values obtained with the model and experimental measurements could be explained by both experimental limitations and model approximations.

1. Introduction

Solid State Nuclear Track Detectors (SSNTDs) can be used to register neutron induced tracks, and the mapping of particle emitting elements is one of their outstanding applications [6]. In particular, they can be employed to determine the local distribution of ^{10}B atoms in different materials [3], tissue samples taken from subjects treated with Boron Neutron Capture Therapy (BNCT) being a case of interest in the field [8,1].

Ion irradiation of non-conducting polymers produces a modification of the local molecular structure along the ion trajectory, and the intensity of damage decreases radially from the projectile incidence axis to the bulk region of unexposed material. Chemical etching processes can be applied to enlarge the track-damaged region up to a scale visible with optical microscopy, allowing the observation of the revealed tracks. Track pit shape is determined by the bulk rate of attack (v_B or bulk velocity) and the preferential attack rate, v_T, along the particle damaged trail. A commonly used quantity is the track etch rate to bulk etch rate ratio, $V = v_T/v_B$.

Depending on the detector material and the ion characteristics, a detection threshold can be observed for certain experimental conditions [5,2]. Different models were proposed to explain the mechanisms involved in the creation of the damaged region, and a number of associated parameters have been analyzed as possible quantitative measures of the detection threshold [12]. On the other hand, an etching efficiency can be defined as the fraction of tracks intersecting a given surface that are revealed under specified etching conditions. This restriction essentially depends on the incidence angle of the particle on the detector surface: for angles of incidence (measured between the ion trajectory and the detector surface) smaller than the critical angle θ_c

$$\theta_c = \arcsin(1/V) = \arcsin(v_B/v_T) \quad (1)$$

no tracks are expected to be observed [7].

In the case of samples containing ^{10}B, they are placed in contact with the detector and subsequently irradiated with thermal neutrons to produce the capture reaction: $^{10}B(n,\alpha)^7Li$. Therefore, the potentially track-generating particles, together with their corresponding energies and yields are: α particles with 1.47 MeV (93.7%) and 1.77 MeV (6.3%) energies, and ^7Li ions with 0.84 MeV (93.7%) and 1.02 MeV (6.3%). Because discrete tracks can be counted after etching the track detector, it is possible to determine the local concentration of boron through the evaluation of the corresponding number of nuclear tracks. In this way the boron concentration in a tissue section can be quantitatively mapped. However, to make quantification possible, it is necessary to

* Corresponding author. Tel.: +54 011 67727150.
E-mail address: gisaint@cnea.gov.ar (G. Saint Martin).

0168-583X/$ - see front matter © 2011 Elsevier B.V. All rights reserved.
doi:10.1016/j.nimb.2011.08.031

calibrate using a "standard" sample containing a known amount of ^{10}B, to be used as a reference.

Nevertheless the question arises if any material can be used as a reference to evaluate samples with composition other than the standard one. In fact, the medium where the neutron capture reaction occurs determines the energy loss of the produced particles, in their trajectory to the detector surface and consequently the energy with which they arrive. This energy value together with the angle of incidence, condition the possibility of observing the track in the detector under consideration, with a given etching process. In this work we simulate the track formation process on a detector in contact with a sample containing a known concentration of ^{10}B atoms in its volume irradiated with a certain fluence of thermal neutrons. The model is applied to study the possible influence of the sample material on the final value of track density, from a theoretical point of view. Additionally, the predictions of the stochastic model are compared with both analytical calculations and track density measurements from borated aqueous solutions in contact with polycarbonate detectors.

2. Materials and methods

2.1. Stochastic simulation

The whole experiment was modelled taking into account the random character of the production of alpha and lithium particles in a sample of a given material containing a known quantity of boron atoms in a specified volume, using stochastic simulation. A Monte Carlo sampling code BPSS (Boron Particle Stochastic Simulation) v. 1.0 was developed to simulate the random generation of boron neutron capture (BNC) reactions in a three-dimensional slab representing the sample. Particles were scored as "detected" whenever they left the slab with an energy and angle fulfilling certain conditions, imposed by the physics of the detection process. Since at microscopic scale the number of BNC reactions is small given the amount of boron usually uptaken by the cells, the stochastic simulation algorithm was constructed in order to obtain estimators of the mean track densities and other quantities of interest. Appropriate statistical weights were assigned to each detected particle in order to renormalize the averages to the sample's boron content. Symmetry considerations based on the particles' emission directions were also included, accepting particles that were emitted in the opposite direction (otherwise not physically detected) by reflecting the randomly sampled incidence angle. In addition, statistical evaluations of the sampling process were made, with the purpose of achieving a suitable precision level. Geometrical and physical conditions of the process were included in the model: range-energy relations, detector characteristics, critical detection angles, etc. To take into account range, energy and LET (Linear Energy Transfer) of the particles, data were obtained from Ion Stopping and Range tables generated by the SRIM-2008.4[1] code based on the work by Ziegler et al. [13]. The V value for each particle arriving at the detector surface was calculated by the semiempirical relationship stated by Somogyi et al. [12] for polycarbonate (density = 1.2 g cm^{-3}) and PEW etching solution (30 g KOH + 80 g ethyl alcohol + 90 g distilled water) at 70 °C:

$$V = V(\mathrm{REL}) = 1 + 0.096(\mathrm{REL})^{2.82} \quad (2)$$

where REL is the Restricted Energy Loss [4] in (MeV cm^2 mg^{-1}) units. It must be mentioned that LET and REL values are practically identical at the considered energy range. Values of these parameters for the particles at their initial conditions are shown in Table 1. Protons produced in potential capture reactions with ^{14}N atoms in tissue are also included in the table.The developed model was run simulating different sample materials: liver tissue with a known concentration of boron, borated aqueous solutions and boron-doped silicon wafers. In addition, the capability of generating "synthetic" images of tracks was implemented, with the purpose of comparing them with the experimental ones. The BPSS results can be compared under certain conditions with analytical calculations using expressions cited in the literature. The considered analytical equation for the track density ρ [7] is

$$\rho = C(\mathrm{B})\frac{N_v \sigma_B \varphi}{4}(R_\alpha \cos^2\theta_\alpha + R_{\mathrm{Li}} \cos^2\theta_{\mathrm{Li}}) \quad (3)$$

where C(B) is the concentration of boron atoms, N_v is the number of atoms per unit volume, σ_B is the neutron capture cross section, Φ is the thermal neutron fluence, R_α, R_{Li} and θ_α, θ_{Li} are ranges and critical angles of the alpha particles and Li ions respectively. Particle ranges in our calculation are weighted averages that consider the reaction yields.

Table 1
Calculated values of V in polycarbonate using expressions by Somogyi et al. [12]. LET and Range values in polycarbonate were obtained with SRIM code for particles at initial conditions. The $V = v_T/v_B$ value calculated for protons is almost equal to 1, so there is essentially no preferential attack velocity, which makes proton tracks not visible.

Particle	Energy (keV)	LET (MeV cm^2/mg)	Range (μm)	V
$Alpha_0$	1770	1.6588	8.24	1.400
$Alpha_1$	1470	1.8069	6.769	1.509
Li_0	1016	3.7424	3.815	4.968
Li_1	840	3.5566	3.396	4.437
H+	580	0.3438	9.43	1.005

2.2. Experimental setup

Lexan™ (manufactured by SABIC Innovative Plastics, formerly General Electric Plastics) amorphous polycarbonate films of 250 μm thickness were used as nuclear track detectors. To evaluate track density production by borated solutions, small boxes (Small Lexan Cases, SLCs) of about 100 μl volume, were designed and assembled with Lexan foils [11] and then filled with analytically prepared ^{10}B solutions (99.99% enrichment). In this work, a concentration of 50 μg g^{-1} is used for comparison with calculated results.

Irradiations with thermal neutrons were performed at the RA-3 reactor of the Ezeiza Atomic Center (CAE) with thermal neutron fluences of 10^{11}, 10^{12} and 10^{13} n cm^{-2}. Neutron flux was previously measured using a SPND (Self Powered Neutron Detector) and the uncertainty in the delivered neutron fluence is 8%. During the irradiation of the foils the flux was monitored at certain reference points to check its stability. Thermal neutron field characterization and dosimetry procedures are specified in Miller et al. [9].

The polycarbonate detectors were etched with PEW alkaline solution at 70 °C for 2 min and then rinsed in abundant water. Latent tracks were so amplified up to microscopic level (track diameters ~1 μm). The resulting tracks were observed in the Carl Zeiss MPM 800 Digital imaging system which consists of a light microscope used in bright field mode and a CCD digital camera Sony Exwave HAD. The evaluation of the number of tracks per unit area was achieved with image analysis software [11] over 50 pictures (40×) in each of three samples corresponding to the same condition. Tracks of all visible sizes were taken into account to evaluate the track density. Overlapping tracks were not a major problem in the range of concentrations and fluences here considered. When considering 10^{13} n cm^{-2} neutron fluence, track counting could be made up to about 50 μg g^{-1} boron concentration. However in those

[1] SRIM-2008.4 Code. *Particle Interactions with Matter.* http://www.srim.org/

cases in which track overlapping introduces a non linearity in the response curve, some corrective factors should be applied [10].

3. Results and discussion

BPSS simulations were performed for the above mentioned materials, considering a 50 μg g^{-1} ^{10}B concentration and 10^{12} n cm^{-2} thermal neutron fluence, and the results were compared with the analytical calculation and experimental measurements. Proportionality between code results for other conditions of boron concentration and neutron fluence can be assumed, since the simulations are performed per particle source and the final estimators are scaled with BNC reaction rate. Fluctuations in track density between identical BPSS runs (identical except for the use of different random numbers sequences) were below 0.8% for 300,000 particle histories.

Figure 1 contains a comparison between results obtained with BPSS, analytical calculations and experimental measurements, for aqueous solution.

In Eq. (3) the etching efficiency is taken into account by introducing a corrective factor proportional to $\cos^2\theta_c$, which is calculated using the initial energies of the particles after the capture reaction. If critical angles are not considered ($\cos\theta_c = 1$) BPSS code calculations must converge to analytical ones, and that coincidence (the difference between both results being 0.2%) is observed in the bars corresponding to results obtained without critical angle (WO/Crit. angle). A more realistic result is obtained with the BPSS code when critical angles are considered (W/Crit. angle bars). In this case, the track density calculated with BPSS code differs from the analytical result by 23%. In fact, critical angles are calculated in the code for each generated particle taking into account its particular characteristics (position, residual range, etc.), instead of using common initial conditions for all of them.

The last bar represents the track density experimental mean value. An uncertainty of around 9% is represented, corresponding to factors included in the expression of track density, mostly fluence uncertainties and range straggling. The deviation in track counts is dependent on the registered number of events, that is, it will be smaller when larger fluence or fields of larger area are considered. For the samples corresponding to the condition studied here the standard deviation was 2%. A 95% confidence interval for the mean of the experimental measurements was determined using the measured standard deviation as an estimator of the square root of the variance. This interval does not contain the value calculated by BPSS. In other terms, though these values resulted close beyond expectations, the difference (about 9%) between them was found statistically significant. In the microscope observation process there is always a number of tracks that pass unnoticed and are not included in the count because they are too small, or poorly contrasted. This fact may explain the lower experimental value, for there is no "observation efficiency" included in the computational model, in which all particles reaching the detector within the critical angle are scored. This kind of limitations, as well as the approximations used in the model (semiempirical expressions employed for the calculation of V, for example) could justify the difference between results.

In Fig. 2 the curve resulting from plotting the calculated number of tracks per unit area as a function of sample thickness are displayed. The calculations were performed for 50 μg g^{-1} boron aqueous solution exposed to a thermal neutrons fluence of 10^{12} n cm^{-2}. The model discriminates tracks produced by alpha particles from those originated by Li ions and the resulting densities are also shown in different curves. It can be seen that track density increases up to a saturation value which is attained by samples with thicknesses greater than 7 μm. On the other hand the number of tracks corresponding to Li ions is higher than that corresponding to alpha particles for samples with thickness under 3.5 μm. For thicker samples the fraction of alpha particles' tracks exceeds the amount attributed to Li ions.

This behaviour is closely related to both the ranges and the critical angles (defined in terms of the V values) of these particles. In Fig. 3, the V value calculated for Lexan, is plotted as a function of the energy for alpha particles and Li ions. The particles arriving to the detector surface have energy values that depend on the distance covered in the sample, which will determine their capacity to be etched.

Figure 4a and c are microphotographs of the tracks in Lexan detectors produced by BNC reactions in 50 μg g^{-1} boron aqueous solution exposed to 10^{11} and 10^{13} n cm^{-2} fluences respectively, obtained in the light microscope. Figure 4b and d correspond to BPSS simulations for the same experimental conditions. Representations of registered tracks in the simulated detector are generated by sampling a Poisson distribution with mean equal to the product of the detector area and the track density estimator (obtained after running the code to simulate a given sample material and detection conditions), producing a dimensionless quantity correspond-

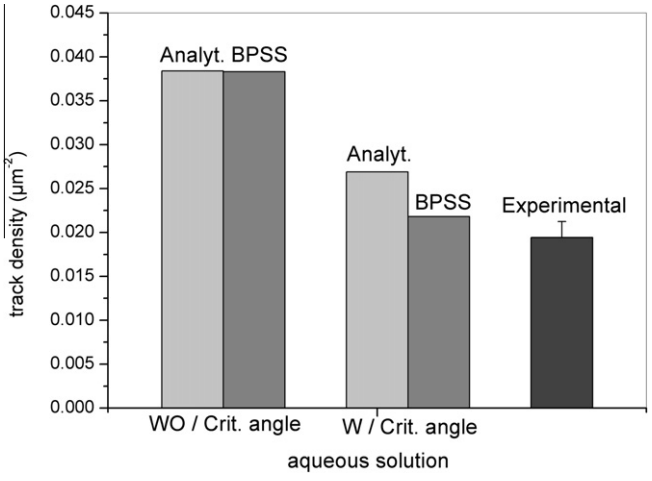

Fig. 1. Track density values obtained by BPSS v.1.0 code, analytical calculation and experimental measurements for 50 μg g^{-1} ^{10}B aqueous solution in Lexan SLCs irradiated with 10^{12} n cm^{-2} thermal neutron fluence. WO: without. W: with.

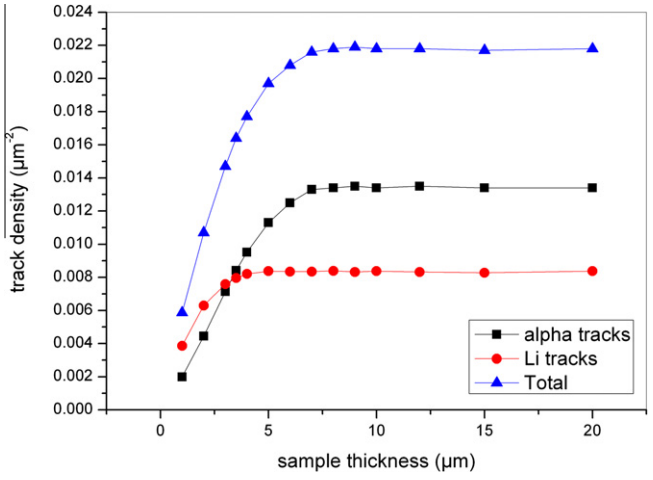

Fig. 2. Calculated number of tracks per unit area produced by 50 μg g^{-1} boron aqueous solution exposed to 10^{12} n cm^{-2} thermal neutrons fluence. Tracks produced by alpha particles and Li ions are shown in different curves, in addition to the total number of tracks.

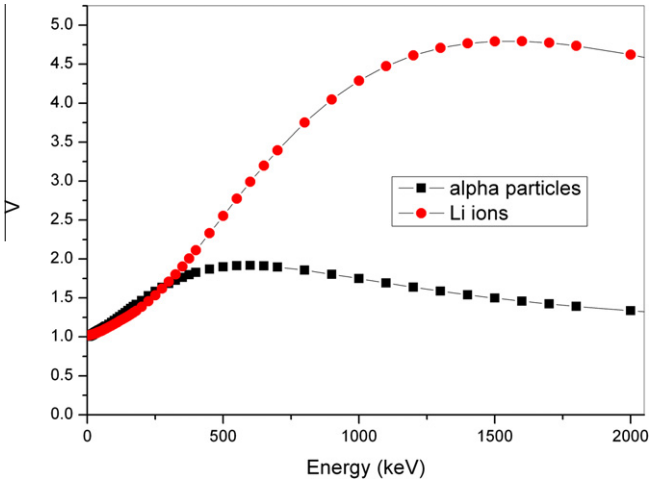

Fig. 3. V value as a function of the energy, for He and Li ions arriving to the polycarbonate detector surface.

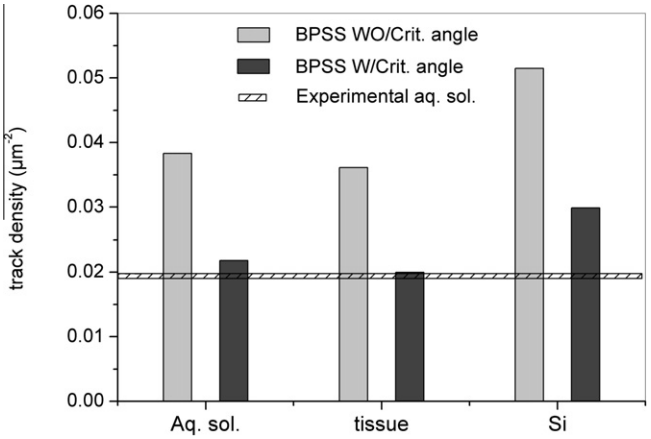

Fig. 5. Track density values in Lexan obtained by BPSS code for 10^{12} n cm^{-2} thermal neutron fluence and 50 μg g^{-1} ^{10}B concentration in: aqueous solution, tissue and Silicon. The horizontal bar represents the 95% confidence interval.

ing to the expected average number of tracks produced in the simulated detector area.

Once the number of tracks is obtained, each track is placed randomly with uniform probability over a two-dimensional region representing the detector area, generating a synthetic image that represents a possible experimental outcome. The size of each point is chosen to represent the average dimensions of an etched pit as seen under the light microscope, and is sketched as an open circle to easily observe overlapping tracks.

It must be stressed that these synthetic images are obtained "a posteriori" of the Monte Carlo simulation, which produces an estimator of the track density with the desired precision and takes into account the physics of the detection process.

It can be noticed that simulated and experimental images are alike. This fact emphasizes the randomness of the whole process, paving the way for better analyzing autoradiography images associated with tissue samples.

Figure 5 shows a comparison between results obtained with the BPSS code for the three materials mentioned above.

It can be seen that the calculated values for aqueous solution and tissue are similar, and the difference factor between them is of the order of the tissue density (here considered as 1.06 g cm^{-3}),

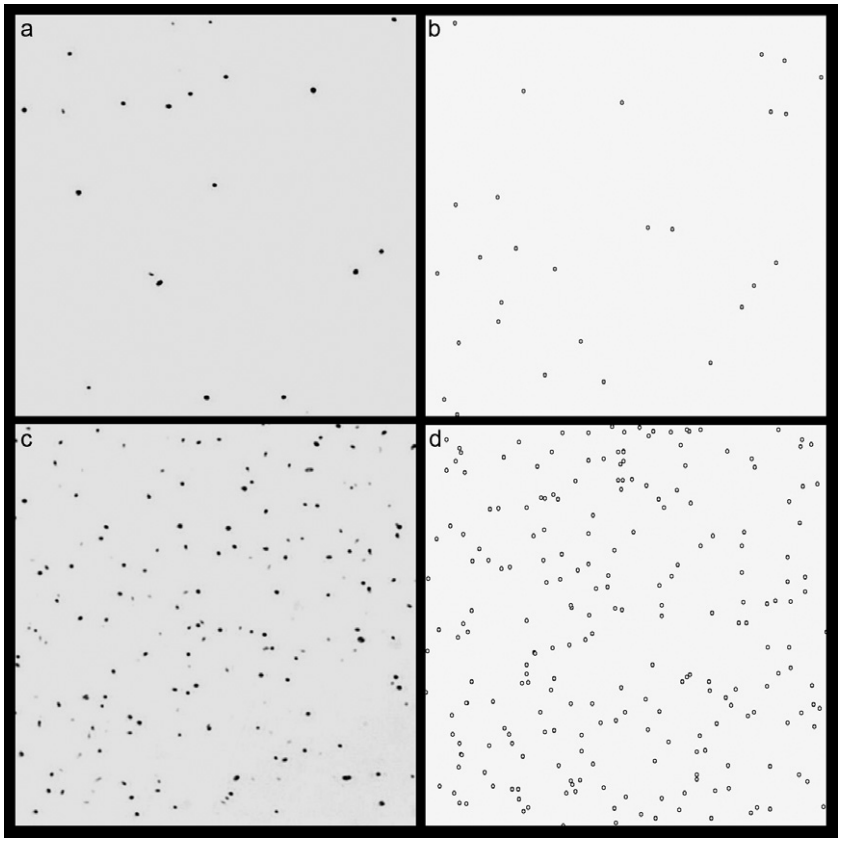

Fig. 4. 100 × 100 μm^2 Experimental (a and c) and synthetic (b and d) images of tracks produced by 50 μg g^{-1} boron aqueous solution in Lexan detectors. (a and b) correspond to 10^{11} n cm^{-2} fluence while (c and d) correspond to 10^{13} n cm^{-2} fluence.

Table 2
Ranges (in 10^{-4} g cm^{-2}) of He and Li ions at the initial energies after capture reaction, for water (aqueous solution), tissue and silicon.

Particle	Energy (keV)	Range (10^{-4} g/cm^3)		
		Water	Tissue	Silicon
$Alpha_0$	1770	9.390	9.551	14.670
$Alpha_1$	1470	7.757	7.886	11.952
Li_0	1016	4.632	5.003	6.523
Li_1	840	4.162	4.494	5.710
Weighted mean range		12.051	12.518	17.884

at most 9%, when critical angles are considered. On the other hand, the differences between values calculated for silicon and aqueous solution and tissue are 37% and 50% respectively, for the same condition. Other variables besides the silicon density value (2.32 g cm^{-3}) seem to be more significant in this case, to explain them. Factors related with the sample composition and the interaction process between the particles and the sample atoms and taken into account through the residual ranges at the detector surface (i.e., atomic number) could be mentioned. The obtained results would support the fact that a reference material cannot be taken as "universal" unless some correcting factors are applied. In this sense the reference system could be used to evaluate samples of materials with a different composition whenever it is possible to assume that the range (in g cm^{-2}) of the track producing particle in the standard and in the sample is virtually the same [6]. Ranges (in g cm^{-2}) for the three considered materials are shown in Table 2. It can be seen that water and tissue values are very close, especially for alpha particles, whilst ranges in Si at the same energies are quite different, particularly for alpha particles.

4. Conclusions

The new Monte Carlo model reproduces the physical conditions of the system as well as the analytical results, which had not been developed until now. Results of track density obtained with the code are close to experimental measurements in Lexan detectors beyond expectation. Limitations in the model to simulate all experimental facts (observation efficiency, for example) as well as the use of certain semiempirical expressions in the calculation, could justify the difference between them.

The actual model permitted an estimation of the particle's proportion depending on the sample thickness. These results allow further analysis in order to theoretically determine the more appropriate thickness to work with, according to the experiment to be performed. This code could also be adapted in order to simulate problems which involve different emitters other than the ^{10}B atoms that form the autoradiography image.

It could be verified that a borated aqueous solution can be used as a reference system for the evaluation of ^{10}B concentration in tissue samples, whenever the particles ranges (in g cm^{-2}) are similar for both materials.

To understand the degree of overlapping between tracks in the SSNTD, one possibility is to analyze the interdistance distribution between track centers from the synthetic images as a function of the neutron fluence and boron concentration. Although not presented in this work, this is one of the future evaluations, which could also include observational efficiency, among other factors.

In addition, future work will focus on the distribution of "random clustering", i.e., the production of clusters of random points in a homogeneous Poisson process, both from the theoretical and the probabilistic point of views. This approach would offer a suitable estimation of their likelihood, essential to preclude "apparent local concentrations" of boron reactions, which could give the false impression of higher boron content in certain regions of the sample, particularly when those regions are superimposed to histological structures.

Acknowledgments

The authors are grateful to Lic. E. Pozzi and Lic. S. Thorp for samples irradiation and to Dr. Sara J. González for her useful comments and suggestions. The digital image analysis was performed at the Lanais MEF (CNEA-CONICET) laboratory. This work was partially supported by Grant PAE 22393, ANPCyT.

References

[1] S. Altieri, S. Bortolussi, P. Bruschi, P. Chiari, F. Fossati, S. Stella, U. Prati, L. Roveda, A. Zonta, C. Zonta, C. Ferrari, A. Clerici, R. Nano, T. Pinelli, Neutron autoradiography imaging of selective boron uptake in human metastasic tumours, Appl. Radiat. Isotopes 66 (2008) 1850–1855.
[2] P.Yu. Apel, D. Fink, Ion Track Etching, in: D. Fink (Ed.), Transport Process in Ion Irradiated Polymers, first ed., Springer, 2004.
[3] J.S. Armijo, H.S. Rosenbaum, Boron detection in metals by alpha-particle tracking, J. Appl. Phys. (5) (1967) 2064–2069.
[4] E.V. Benton. Charged particle tracks in polymers. No. 4: Criterion for track registration. US Naval Radiological Defense Laboratory, San Francisco, Report USNRDL-TR-67-80 (1967).
[5] O.A. Bernaola, G. Saint-Martin, C. Grasso, Detection threshold in polymers, Nucl. Tracks Radiat. Meas. (1–4) (1994) 25–28.
[6] S.A. Durrani, R.K. Bull, Solid State Nuclear Track Detection. Principles, Methods and Applications, in: D. ter Haar (Ed.), International Series in Natural Philosophy, Pergamon Press, 1987.
[7] R.L. Fleischer, P. Price, R.M. Walker, Nuclear Tracks in Solids, University of California Press, Berkeley, 1975.
[8] W.S. Kiger, P.L. Micca, G.M. Morris, J.A. Coderre, Boron microquantification in oral mucosa and skin following administration of a neutron capture therapy agent, Radiat. Prot. Dosim. 99 (1-4) (2002) 409–412.
[9] M. Miller, J. Quintana, J. Ojeda, S. Langan, S. Thorp, E. Pozzi, M. Sztejnberg, G. Estryk, R. Nosal, E. Saire, H. Agrazar, F. Graiño, New irradiation facility for biomedical applications at the RA-3 reactor thermal column, Appl. Radiat Isot. 67 (7-8 Suppl) (2009) S226–S229.
[10] J.P. Pignol, J.C. Abbe, M. Thellier, A. Stampfler, Neutron capture radiography applied to the investigation of boron-10 biodistribution in animals: improvements in techniques of imaging and quantitative analysis, Nucl. Instr. Meth. B 94 (4) (1994) 516–522.
[11] A. Portu, M. Carpano, A. Dagrosa, S. Nievas, E. Pozzi, S. Thorp, R. Cabrini, Reference systems for the determination of ^{10}B through autoradiography images: set up and application to a melanoma experimental model, Proceedings of 14th International Congress on Neutron Capture Therapy, October 25–29, 2010. Buenos Aires, Argentina (2010) 287–290.
[12] G. Somogyi, K. Grabisch, R. Scherzer, W. Enge, Revision of the concept of registration threshold in plastic track detectors, Nucl. Instr. Meth. 134 (1976) 129–141.
[13] J.F. Ziegler, J.P. Biersack, U. Littmark, The Stopping and Range of Ions in Matter, Pergamon Press, New York, 1985.